



AFRL-AFOSR-VA-TR-2016-0381

Iodine Plasma (Electric Propulsion) Interaction with Spacecraft Materials

**Richard Branam
UNIVERSITY OF ALABAMA
301 ROSE ADMINISTRATION BLDG
TUSCALOOSA, AL 35487-0001**

**12/28/2016
Final Report**

DISTRIBUTION A: Distribution approved for public release.

Air Force Research Laboratory
AF Office Of Scientific Research (AFOSR)/RTA1

REPORT DOCUMENTATION PAGE					<i>Form Approved OMB No. 0704-0188</i>							
The public reporting burden for this collection of information is estimated to average 1 hour per response, including the time for reviewing instructions, searching existing data sources, gathering and maintaining the data needed, and completing and reviewing the collection of information. Send comments regarding this burden estimate or any other aspect of this collection of information, including suggestions for reducing the burden, to the Department of Defense, Executive Service Directorate (0704-0188). Respondents should be aware that notwithstanding any other provision of law, no person shall be subject to any penalty for failing to comply with a collection of information if it does not display a currently valid OMB control number.												
PLEASE DO NOT RETURN YOUR FORM TO THE ABOVE ORGANIZATION.												
1. REPORT DATE (DD-MM-YYYY) 05-12-2016		2. REPORT TYPE Final			3. DATES COVERED (From - To) 15-09-2015 to 14-09-2016							
4. TITLE AND SUBTITLE Iodine Plasma (Electric Propulsion) Interaction with Spacecraft Materials				5a. CONTRACT NUMBER FA9550-15-1-0371								
				5b. GRANT NUMBER 15-0505								
				5c. PROGRAM ELEMENT NUMBER								
6. AUTHOR(S) Richard D. Branam				5d. PROJECT NUMBER								
				5e. TASK NUMBER								
				5f. WORK UNIT NUMBER								
7. PERFORMING ORGANIZATION NAME(S) AND ADDRESS(ES) The University of Alabama Office for Sponsored Programs 152 Rose Admin. Bldg. Box 870104					8. PERFORMING ORGANIZATION REPORT NUMBER							
9. SPONSORING/MONITORING AGENCY NAME(S) AND ADDRESS(ES) <div style="display: flex; justify-content: space-between;"> <div style="width: 45%;"> Air Force Office of Scientific Research Dr. Mitat A. Birkan AFOSR/RTE E-mail: mitat.birkan@us.af.mil Phone: (703) 696-7234 </div> <div style="width: 45%;"> Air Force Office of Scientific Research 875 North Randolph Street Suite 325, Room 3112 Arlington VA, 22203 </div> </div>					10. SPONSOR/MONITOR'S ACRONYM(S)							
					11. SPONSOR/MONITOR'S REPORT NUMBER(S)							
12. DISTRIBUTION/AVAILABILITY STATEMENT DISTRIBUTION A: Distribution approved for public release.												
13. SUPPLEMENTARY NOTES												
14. ABSTRACT Initial mission profile studies have shown iodine will enable micro-satellites to accomplish several Air Force missions using much smaller, cheaper satellites; orbit raising, deorbiting, rendezvous, maintenance mission, orbital debris removal, retrieval of errant spacecraft. Iodine imparts volume-constrained spacecraft with up to three times the impulse compared to existing space propulsion systems (i.e. Hall Effect Thruster with xenon). Iodine is stored as a solid (no high pressure vessels), at density three times those of xenon (impulse density two to three times). Iodine presents unique challenges, though. This research addressed the impact of iodine on solar panel surfaces, spacecraft structures and sensitive instruments on board satellites by providing predictive computational tools to satellite designers. Accumulation of iodine film on spacecraft surfaces will present several unique issues: chemical erosion and iodine adsorption/absorption. Of particular concern would be shorting dielectric surfaces, changing radiator emissivities, and damaging optical coatings. To date, chemical reactivity and chemical erosion of iodine with several satellite materials (steel, aluminum, tantalum, etc.) have been determined and tested.												
15. SUBJECT TERMS iodine, space, propulsion, ion propulsion, electric propulsion, propellant												
16. SECURITY CLASSIFICATION OF: <table border="1" style="width: 100%; border-collapse: collapse;"> <tr> <td style="width: 33%; padding: 2px;">a. REPORT</td> <td style="width: 33%; padding: 2px;">b. ABSTRACT</td> <td style="width: 33%; padding: 2px;">c. THIS PAGE</td> </tr> <tr> <td style="text-align: center; padding: 2px;">UU</td> <td style="text-align: center; padding: 2px;">UU</td> <td style="text-align: center; padding: 2px;">UU</td> </tr> </table>			a. REPORT	b. ABSTRACT	c. THIS PAGE	UU	UU	UU	17. LIMITATION OF ABSTRACT <div style="text-align: center; padding: 5px;">UU</div>		18. NUMBER OF PAGES	
a. REPORT	b. ABSTRACT	c. THIS PAGE										
UU	UU	UU										
					19a. NAME OF RESPONSIBLE PERSON Richard D. Branam							
					19b. TELEPHONE NUMBER (Include area code) 205-348-3233							

INSTRUCTIONS FOR COMPLETING SF 298

1. REPORT DATE. Full publication date, including day, month, if available. Must cite at least the year and be Year 2000 compliant, e.g. 30-06-1998; xx-06-1998; xx-xx-1998.

2. REPORT TYPE. State the type of report, such as final, technical, interim, memorandum, master's thesis, progress, quarterly, research, special, group study, etc.

3. DATES COVERED. Indicate the time during which the work was performed and the report was written, e.g., Jun 1997 - Jun 1998; 1-10 Jun 1996; May - Nov 1998; Nov 1998.

4. TITLE. Enter title and subtitle with volume number and part number, if applicable. On classified documents, enter the title classification in parentheses.

5a. CONTRACT NUMBER. Enter all contract numbers as they appear in the report, e.g. F33615-86-C-5169.

5b. GRANT NUMBER. Enter all grant numbers as they appear in the report, e.g. AFOSR-82-1234.

5c. PROGRAM ELEMENT NUMBER. Enter all program element numbers as they appear in the report, e.g. 61101A.

5d. PROJECT NUMBER. Enter all project numbers as they appear in the report, e.g. 1F665702D1257; ILIR.

5e. TASK NUMBER. Enter all task numbers as they appear in the report, e.g. 05; RF0330201; T4112.

5f. WORK UNIT NUMBER. Enter all work unit numbers as they appear in the report, e.g. 001; AFAPL30480105.

6. AUTHOR(S). Enter name(s) of person(s) responsible for writing the report, performing the research, or credited with the content of the report. The form of entry is the last name, first name, middle initial, and additional qualifiers separated by commas, e.g. Smith, Richard, J, Jr.

7. PERFORMING ORGANIZATION NAME(S) AND ADDRESS(ES). Self-explanatory.

8. PERFORMING ORGANIZATION REPORT NUMBER.

Enter all unique alphanumeric report numbers assigned by the performing organization, e.g. BRL-1234; AFWL-TR-85-4017-Vol-21-PT-2.

9. SPONSORING/MONITORING AGENCY NAME(S) AND ADDRESS(ES). Enter the name and address of the organization(s) financially responsible for and monitoring the work.

10. SPONSOR/MONITOR'S ACRONYM(S). Enter, if available, e.g. BRL, ARDEC, NADC.

11. SPONSOR/MONITOR'S REPORT NUMBER(S). Enter report number as assigned by the sponsoring/monitoring agency, if available, e.g. BRL-TR-829; -215.

12. DISTRIBUTION/AVAILABILITY STATEMENT. Use agency-mandated availability statements to indicate the public availability or distribution limitations of the report. If additional limitations/ restrictions or special markings are indicated, follow agency authorization procedures, e.g. RD/FRD, PROPIN, ITAR, etc. Include copyright information.

13. SUPPLEMENTARY NOTES. Enter information not included elsewhere such as: prepared in cooperation with; translation of; report supersedes; old edition number, etc.

14. ABSTRACT. A brief (approximately 200 words) factual summary of the most significant information.

15. SUBJECT TERMS. Key words or phrases identifying major concepts in the report.

16. SECURITY CLASSIFICATION. Enter security classification in accordance with security classification regulations, e.g. U, C, S, etc. If this form contains classified information, stamp classification level on the top and bottom of this page.

17. LIMITATION OF ABSTRACT. This block must be completed to assign a distribution limitation to the abstract. Enter UU (Unclassified Unlimited) or SAR (Same as Report). An entry in this block is necessary if the abstract is to be limited.

Iodine Plasma (Electric Propulsion) Interaction with Spacecraft Materials

Richard D. Branam, PhD
Principle Investigator
Assistant Professor of Aerospace Engineering
rdbranam@eng.ua.edu

Start Date: September 15, 2015

End Date: September 14, 2016

Submitting Institution – The University of Alabama
801 University Blvd.
Tuscaloosa, AL 35487

Broad Area Announcement, Air Force Office of Scientific Research -- BAA-AFOSR-2014-0001

Iodine as an Alternative Fuel for Electric Propulsion

Research Objective

This research will provide satellite designers with the needed materials-interaction information to use iodine as a propellant.

Current electric satellite thrusters employ xenon propellant stored in high pressure tanks limiting the amount of total impulse available to the satellite. Iodine is stored as a solid (no high pressure vessels), at density three times those of xenon (impulse density two to three times). The increase in total impulse for a small satellite will enable the satellite to reach the Moon and other near Earth objects. Iodine presents unique challenges, though.

This report is submitted as a final report for the first year of research effort as well as the work planned for a second and third year to provide verifiable, valid results with significance to the satellite designer.

In this first year (Sep 2015 – Sep 2016), the research addressed the impact of iodine on a sampling of spacecraft materials (aluminum, copper, and iron alloys). The exposure process was validated and is ready to extend to the remaining satellite materials. A materials list of exposed satellite materials has been created.

The second year, the research will extend the effort to expose solar panel surfaces, spacecraft structures and sensitive instruments on board satellites to iodine and iodine plasma. The research will continue to quantify the compatibility of iodine by focusing on the reactivity processes (both chemical kinetics and thermodynamic) on the various spacecraft surfaces.

The third year of research will continue to characterize the sputter/erosion interactions. Sputter and erosion interactions will be quantified to compare with xenon models as well as update the momentum-exchange, empirical models used today.

Technical Approaches

1. Measure iodine impact (chemical compatibility, erosion) on spacecraft materials
2. Measure impact of iodine plasma in space-like conditions.
3. Develop iodine-interaction models for spacecraft materials (chemical reactivity, sputtering, and erosion)

Impact of Research

Iodine is stored as a solid at a density three times that of xenon (increasing potential delta-V density) and is 25,000 times more abundant, making it a desired replacement, especially for volume-constrained payloads.

Initial mission profile studies have shown iodine will enable micro-satellites to reach the Moon and other Near Earth Objects (NEOs). The use of iodine enables spacecraft to be capable of surveying asteroids for mineral mining at a fraction of the cost of today's interplanetary missions. By imparting volume-constrained spacecraft with up to three times the delta-V, several Air Force missions become possible using much smaller, cheaper satellites; orbit raising, deorbiting, rendezvous, maintenance mission, orbital debris removal, retrieval of errant spacecraft.

Table of Contents

Research Effort	1
Relevance to the Air Force	1
Technical Approach	2
Background	2
Iodine as Propellant.....	3
Progress to Date	2
Spacecraft Iodine Environment.....	3
Inside Cathode	3
Exhaust Plume	5
Spacecraft Exposure.....	7
Iodine Feed System.....	8
Technical Approach	9
Iodine Impact and Iodine Plasma in Space-Like Conditions.....	9
Sputtering Impacts of Iodine.....	14
Experimental Setup	14
Iodine and Iodine Plasma.....	14
Experimental Iodine Feed System	15
Plasma Generation	15
Verifiably Measuring Plasma Properties	16
Momentum Exchange (Sputtering).....	17
Collaboration.....	18
References and Citations.....	19

Research Effort

This overall research will provide satellite designers with the needed modelling tools and an advanced non-intrusive laser diagnostic to use iodine as a propellant.

US Hall Effect Thruster (HET) technology has matured to an operational level, but has not yet become a mainstream propulsion solution for manufacturers or deep space researchers. HET devices do not provide superior system level performance when compared to existing propulsion systems, but using iodine as a propellant eliminates this shortfall.

Current HET's employ xenon propellant as have most deployed electric propulsion devices. Xenon offers many advantages: high atomic mass, low ionization energy, no toxicity, long term (albeit high pressure) storage, material compatibility. Xenon is a very expensive substance, though, and is not mined in high quantity. As of 2001, roughly ten tons of xenon is produced in a year.¹ This limited supply cannot sustain current industry demand (automotive headlights) and future space systems. Iodine is a much cheaper alternative than xenon, 25,000 times more abundant in the Earth's crust.⁵

Recent HET iodine testing has shown comparable performance to xenon. Of significant advantage is the overall system level performance increases iodine offers. Iodine has a higher storage density and resulting higher ΔV capability for volume-constrained systems. Iodine's low vapor pressure permits low-pressure storage and minimizes potential adverse spacecraft-thruster interactions. The iodine will not condense inside the thruster at ordinary operating temperatures and pressures.³

Relevance to the Air Force

NASA has begun work on qualifying a flight-like propellant delivery system and two HET devices for iodine. Work is underway to qualify cathodes using iodine. Busek Co., Inc. is provided engineering models of the hardware to begin testing in FY15 with plans to launch a satellite with iodine propellant in FY17. Several unknowns have been identified and need further testing: material compatibility, spacecraft/plume interactions, sputter erosion, erosion modeling and lifetime analyses. Research has considered the impact of using xenon propellant, but little is known about the impact of iodine. The difference in solar panel surface erosion and impact to sensitive instruments on board satellites needs to be determined.

Accumulation of iodine film on spacecraft surfaces could present several unique issues such from un-ionized neutral iodine. Of particular concern would be shorting dielectric surfaces, changing radiator emissivities, and damaging optical coatings. Specifically, rates of material sputtering, exhaust flux levels and material deposition will erode antennas, instruments and solar arrays, deteriorating their performances. These phenomena will be quantified and incorporated into existing satellite design tools. The anticipated outcome is to suggest certain spacecraft material choices or coatings to be used when employing iodine as the propellant.

Initial mission profile studies have shown iodine will enable micro-satellites to reach the Moon and other Near Earth Objects (NEOs). The use of iodine enables spacecraft to be capable of surveying asteroids for mineral mining at a fraction of the cost of today's interplanetary missions. By imparting volume-constrained spacecraft with up to three times the delta-V, several Air Force mission become possible using much smaller, cheaper satellites; orbit raising, deorbiting, rendezvous, maintenance mission, orbital debris removal, retrieval of errant spacecraft.

Technical Approach

1. Measure iodine impact (chemical compatibility, erosion) on spacecraft materials
2. Measure impact of iodine plasma in space-like conditions.
3. Develop iodine-interaction models for spacecraft materials (chemical reactivity and sputtering
→ total loss of material)

Background

Cost, performance, and efficiency are the primary focus factors in the field of space propulsion. Increased performance and efficiency for spacecraft propulsion systems is best referred to as mass efficiency. The less propellant mass needed to maintain or change orbits in space, the more payload mass is able to be on orbit. In addition to reduced mass, higher electrical efficiency specific to in-space propulsion reduces the demands of the power subsystem, which also decreases mass and cost of a satellite.² Iodine has the potential to provide a significantly more efficient propulsion solution.

NASA continues its investment in iodine based Hall Effect Thruster (HET) systems to capture two distinct mission niches; very-low power small satellites and high-power exploration class electric propulsion.³ The iodine Satellite (iSAT) Hall Thruster Demonstration Mission is currently developing hardware to support FY17 and FY18 satellite space experiment launches.³ The expected iodine exposure expected by the iSAT will be used to define the testing conditions for this research.

The very-low power satellites are volume and power limited (i.e. CubeSats). The iSAT project intends to mature iodine, ion-thruster technology to enable high ΔV primary propulsion for NanoSats (1-10kg), MicroSats (10-100kg) and MiniSats (100-500kg) with their flight demonstration.³

The iSAT spacecraft configuration has gone through several revisions but the basic plume interactions will be similar. A 12U cubesat (Figure 1) with the solar panels deployed as far away as practical from the thruster and the plume provides protection for these surfaces from propellant interactions.

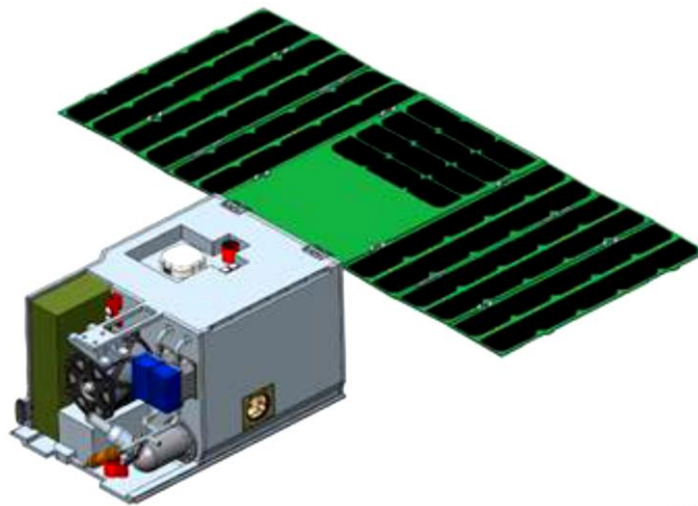


Figure 1: iSAT Configuration Modeled⁴

Iodine as Propellant

A quick comparison of required spacecraft volume for propellant tanks shows how iodine is advantageous for missions requiring extensive maneuvering (Figure 2). For a notional long-term mission requiring large quantities of propellant, the volume of the iodine tanks will be 1/3 the volume of the comparable xenon tanks (higher xenon density is possible than just 1.6 kg/l but then cryogenic storage is necessary). Additionally, the iodine has the advantage of being stored at moderate temperatures and pressures, reducing the demand for high-pressure tanks and plumbing. Iodine enables the potential for ‘fitting’ the tanks to the volume available in a spacecraft using additive manufacturing as well (no domes or composites are needed).

Lower ionization potential demands less energy on the spacecraft. Further evidence is shown in Figure 3. The ionization cross section corresponds directly to probability of an atom being ionized. Iodine is clearly more likely to be ionized than xenon at electron energies between 10eV and 200eV. This means for a given power setting, more iodine will be ionized (increased current) and available to propel the vehicle. Increasing current flow directly increases thrust. With xenon and iodine having very similar molecular masses and iodine being 15 times more likely to ionize, the thrust would be increased overall in an iodine propellant system.

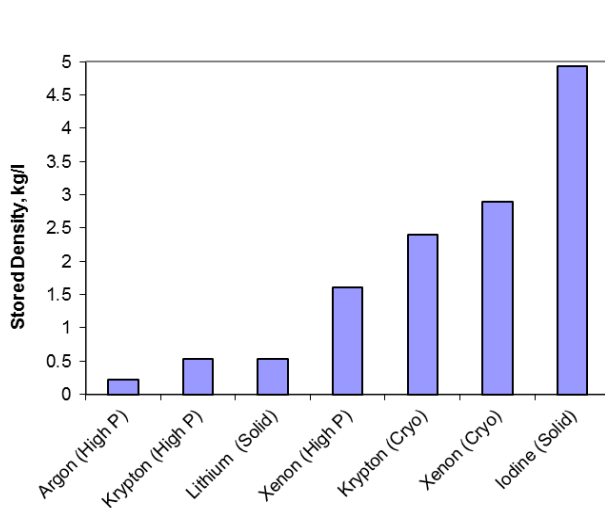


Figure 2: Stored Density of Electric Rocket Propellants in kg/l (high pressure at 14-MPa, 50°C).³

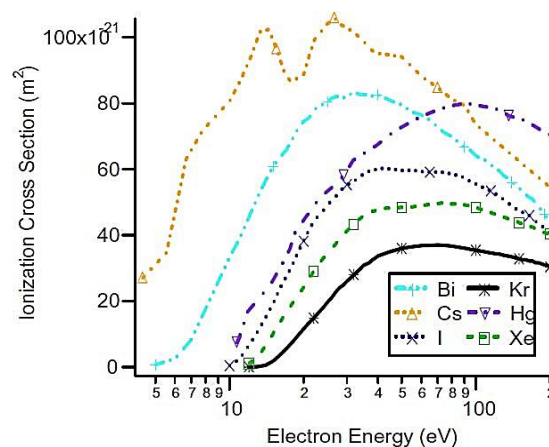


Figure 3: Ionization Cross Sections for Various Hall Thruster Propellants¹

Iodine introduces a reactivity issue. Reactivity is affected by physical properties (i.e. surface properties) thermodynamics (free energy) and kinetics (valance bond theory). In pure substances, increased exposure (surface area) will result in increased reactivity. Thermodynamically, the chances of a reaction of two substances increases if the final products have a lower free energy. According to valance bond theory, the outer shell electrons can help explain the probability of a reaction. The focus of this research is defined by the expected environment found on a satellite with a Hall Effect thruster (physical and thermodynamic) and focused on the specific materials used in satellite manufacture.

Performance of spacecraft propulsions systems have to include total system impact, not just propulsion device performance. Storing propellants at cryogenic temperatures, for example, places

significant demands on the satellite designer resulting in spacecraft power demands, monitoring of the propellant, and propellant conditioning. Iodine is stored as a solid and can be vaporized using very little power. Other prospective propellants have significantly high melting points requiring large amounts of energy and then still need to be vaporized before they can be effectively used.

Iodine is commonly a negative ion in the monatomic state as is typical with halogens. The proven ionization process used by space propulsion devices introduces high energy electrons. These electrons do influence the diatomic iodine to disassociate and create a negative ion in some instances. Negatively charged ions hurt the performance and efficiency of the thruster as the electric field attempts to accelerate negative charges in the wrong direction.⁵ Electronegativity describes the amount of energy needed for the monatom or diatom to capture an electron. The electronegativity of iodine is 2.5 eV for the diatom and 3.0 eV for the monatom, a low number compared to the ionization energies (10.4 eV monatom and 9.4 eV diatom). The iodine is likely to capture electrons and become negative ions. The electric field in the thruster will then force the negative ions in the same direction as the electrons: into the thruster. The Hall Effect (magnetic field) will not significantly influence the negative ions due to their larger relative mass as compared to the swirling electrons. The negative ions will head directly for the anode. By design, the energy of the majority of electrons influencing ionization is significantly more than the electron affinity of iodine. These electrons have too much energy to be captured, reducing the probability of negative ionization. Iodine can potentially outperform the conventional xenon thruster but definitely will require the propulsion device to operate under specific appropriate conditions.

Additionally, the effect of iodine ionizing as a diatom will significantly increase the performance (thrust) as propellant atomic mass increases to 254 amu.²¹ The differences in dissociation energy and ionization energy suggest that monatomic ions will be more prevalent: 1.5 eV to dissociate the diatom and 9.4 eV to ionize the diatom.⁵ The expectation is to see some diatomic ionization, though.²¹

Included in the system impacts is the removal of mass from the spacecraft through momentum exchange. The software tools capture the momentum exchange impact by using the sputtering model created by Kannenberg (Equation 1).⁶ The sputter yield (Y) is a function of the energy of the particles impacting the surface (E) and the angle the particle impacts the surface (θ). The coefficients are material dependent (c_1, c_2, c_3, c_4, c_5). Currently, values are available for xenon ions (singly ionized) and neutrals. Values for iodine need to be determined in a manner to ensure the model correctly handles the chemical reaction losses and momentum erosion (sputtering).

$$Y(E, \theta) = (c_1 + c_2 E)(c_3 \cos \theta + c_4 \cos^2 \theta + c_5 \cos^3 \theta) \quad [1]$$

Progress to Date

The progress achieved during the first year include substantial achievements in characterizing the iodine interactions.

This research effort is being support by a satellite domain modeling effort (COLISEUM modeling) to accurately identify the needed exposure levels and energy states of iodine plasma on a spacecraft. Space vehicle modeling efforts are currently being supported by a subcontracted effort with Busek, Co., Inc. through an STTR, “Unmanned Solar Electric Resource Prospector.” Model results show the most significant iodine concentrations will impact the thruster and the solar

panels. The results for the prospector show a need to consider iodine concentrations and pressures as high as 1.0×10^{16} and 0.1 Pa, respectively.⁷

Progress is being made measuring iodine impact on spacecraft materials. Dr. Branam worked with NASA/MSFC over the summer through a faculty fellowship. While at the Marshall Space Flight Center, Dr. Branam worked to build up the capabilities of the materials sciences directorate (EM-31) to test iodine and iodine plasma interactions. His Ph.D. student mirrored his efforts at the University of Alabama lab facilities.

The results thus far include exposing several materials to iodine at low and moderate pressures and the construction of an iodine plasma chamber. A surprising result from the iodine exposure is the lower oxidation resistance of the refractory metals. Tungsten and tantalum both showed significant loss due to iodine compound formations.

Spacecraft Iodine Environment

The initial studies and the first year's effort have identified four exposure environments of interest for the spacecraft interaction testing (Table 1). The main parameters needed to be established for the exposure environments are pressure, iodine density, iodine plasma density and test article temperature. The following table provides a summary of these parameters, based on the identified exposure environments.

Table 1: Material Testing Environments

Exposure Environment	Pressure (Pa)	Iodine Density (#/m³)	Iodine Plasma Density (#/m³)	Test Article Temperature
Inside cathode	300	6.58×10^{21}	2.5×10^{20}	1900 K (LaB ₆)
Exhaust plume	0.1	10^{14}	10^{18}	500 K
Spacecraft exposure	0.001	10^{14}	1.64×10^{16}	298 K (248 to 473 K)
Iodine feed system	10,000 Pa	2.63×10^{22}	N/A	473 K

Inside Cathode

Cathodes have three commonly utilized insert materials in current state-of-the-art cathodes. Lanthanum hexaboride (LaB₆) and cerium hexaboride (CeB₆) have bulk work functions near 2.7 eV and 2.5 eV, respectively.^{8,9} Barium-impregnated porous tungsten (BaO-W) has a work function of 2.1 eV.⁸ To start the cathode, BaO-W inserts must be heated to 1300 K, and LaB₆ inserts to 1900 K.⁸ A room-temperature, stable electride (12CaO*Al₂O₃:(4e-)) has shown in testing the ability to produce electrons while resisting any corrosion or interaction from the iodine and iodine plasma. The CSU electride produced current as high as 0.15 A/m², temperature of 50 °C.¹⁰ The work function for this material was calculated at 0.76 eV.

The inserts are usually shielded from direct contact with the barrel (Figure 4) using graphite. The insert materials will migrate into the molybdenum or tantalum barrel. The barrel orifice is often made from thoriated or lanthanated tungsten. Some applications replace this expensive material with tantalum as seen in Figure 4. The keeper (graphite, molybdenum or steel) needs to be electrically isolated from the insert. The separation between the keeper and barrel allows for the plasma to migrate toward the heater and shielding. The heater is typically covered with alumina (Al₂O₃) or magnesia (MgO). These ceramics are expected to be fairly resistant to the reactive iodine and iodine plasma. The tantalum heat shielding, though, does react with iodine.

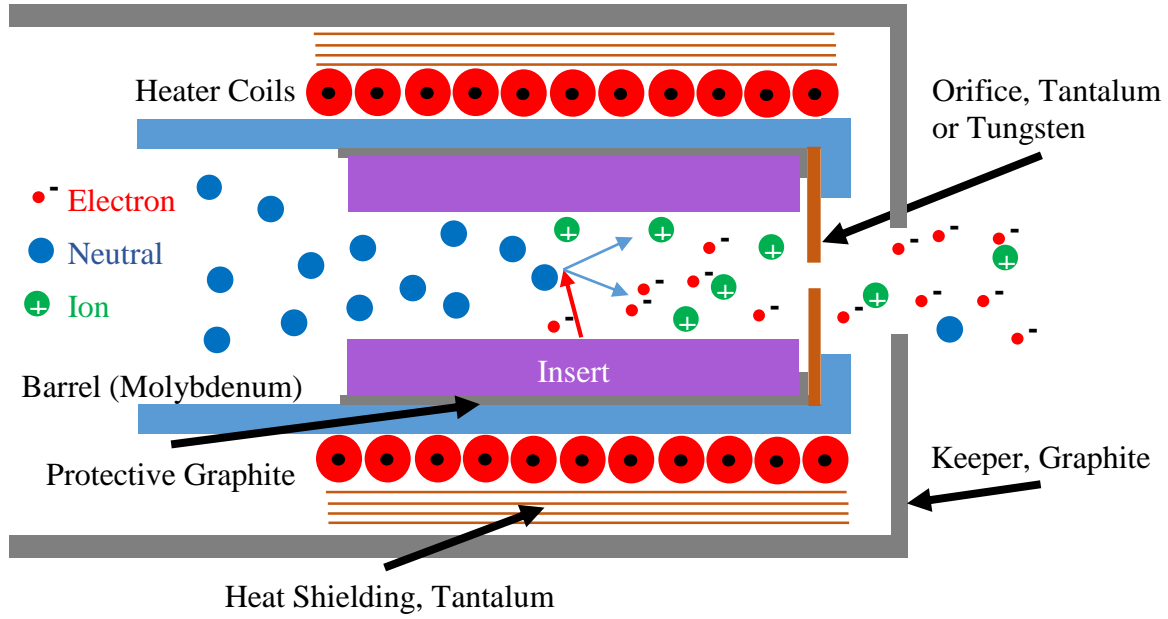


Figure 4: Hollow Cathode Configuration

Determining pressure (and therefore plasma density) inside the cathode can be accomplished using Katz model.^{11,12} Equations 2 through 4 provide the relationships to determine pressure and plasma density. These equations are results from the continuity equation and Poiseuille flow relationships. Equation 2 is the temperature dependent viscosity. The constants in this equation are for xenon. Table 2 provides the values for this research.

$$\begin{aligned} \zeta &= 2.3 \times 10^{-5} T_r^{0.965} & T_r < 1 \\ \zeta &= 2.3 \times 10^{-5} T_r^{(0.71 + \frac{0.29}{T_r})} & T_r > 1 \end{aligned} \quad [2]$$

The relative temperature (T_r) is given by $T_r = T/289.7$ K, units are Pa-s.¹³ Neutral gas temperatures in the insert region are heated by charge exchange. The increase in temperature increases the viscosity. The temperature in equation 2 can be determined from measuring the wall temperature and using the relationship equation 3. Gas temperature can be estimated as three times the wall temperature.¹⁰ The measured wall temperature for our research is 1106 K.

$$T = T_{wall} + \frac{M}{k} [(f v_r)^2 + v_0^2] \quad [3]$$

The pressure is then determined from the pressure drop across the orifice (Poiseuille flow) using viscosity, temperature and flow rate.

$$P = \sqrt{0.78 Q \zeta T_r \left(\frac{l_{orifice}}{d_{orifice}^4} + \frac{L_e}{d_{i,barrel}^4} \right)} \quad [4]$$

The ion density can be determined by the energy lost in the insert, equation 3.¹² For our test conditions, the resulting pressure and ion density are 300 Pa, 2.50×10^{20} ions/m³.

$$n_e = \frac{RI_e^2 - \left(\frac{5}{2}T_{eV} - \phi_s\right)I_e}{\left(f_n T_{eV} \sqrt{\frac{eT_{eV}}{\pi m}} e A e^{\frac{-\phi_s}{T_{eV}}} + n_0 e \langle \sigma_i v_e \rangle V (U^+ + \phi_s)\right)} \quad [5]$$

Table 2: Cathode Pressure and Plasma Density

Q	Flow rate in sccm	10 sccm
T_r	Reduced gas temperature (T _g /298K) ¹	15.3
l_{orifice}	Length of orifice	0.25 mm
L_e	Length of emitter	25.4 mm
d_{orifice}	Orifice diameter	1.0 mm
d_{i,barrel}	Inside diameter of the barrel	8 mm
Pressure	total pressure inside the insert	300 Pa
n₀	Neutral density (P = nkT)	6.58 x 10 ²¹ #/m ³
T_e	Electron temperature	From 2 to 4 eV. ¹¹
n_e	Plasma density	2.50 x 10²⁰ ions/m³.

Exhaust Plume

Spacecraft components exposed to the exhaust plume primarily include the thruster itself. For this research, the Busek BHT-200 Watt Hall Effect Thruster, employed on the iSAT, is used to define the plasma environment. The BHT-200 is a well-known, highly characterized thruster, proven in space missions. It is being used with a BHC-1500 hollow cathode mounted in a standard configuration. The xenon nominal operating condition is 250 volts and 800 milliamps discharge (Table 3).

Table 3: Busek 200W Hall Thruster Operating Conditions

	Xenon	Iodine
Discharge voltage (V)	250	250
Discharge current (A)	0.75	0.74
Anode mass flow rate (mg/s)	0.84	0.82
Cathode mass flow rate (mg/s)	0.098	0.096
Mass (propellant) utilization efficiency	0.981	0.853
Ion mass flow rate (kg/s)	8.24E-07	6.99E-07
Neutral species temperature (K)	500	500

The xenon and iodine plasma exhaust plumes have been modeled using COLISEUM.¹⁴ COLISEUM combines several independently developed modules performing various tasks related to the damage assessment, such as surface and volume specification, plume motion calculation, material properties, and sputter (erosion) rates.¹⁵ Of special interest is AQUILA, which performs Particle-in-Cell Direct Simulation Monte Carlo (PIC-DSMC) calculations to determine the distribution of the plasma.¹⁶ The program requires information about the thruster plasma source: exhaust species, mass flow rates, and temperatures. PIC-DSMC codes account for the thermal non-equilibrium effects of plasma by treating the interaction between the electrons and charged plume

¹ Based on measured wall temperatures of 1196 K. Gas temperature assumed to be three times the wall temperature.¹¹

in either a decoupling or one-way coupling manner due to the disparate time scales between the electrons (10^{-10} s) and plasma (10^{-3} s).^{17,18}

Exhaust particles were modeled in two parts: ions and neutrals.¹⁹ The neutrals were modeled as a Maxwellian distribution at 500 K with a drift velocity of 230 m/s out of the thruster. The information on the ions came from measurements of ion energy distribution (Figure 5) and current density as a function of angle from the centerline of the thruster (Figure 6). The information available on the particle interactions (elastic collisions, charge-exchange collisions) are modeled using collision cross-sections and a probabilistic model. For xenon and iodine in a Hall thruster plume, these cross sections are typically on the order of 10^{-16} cm².²⁰ The COLISEUM model (Figure 5) provided the plume interaction with the thruster as well as with the rest of the spacecraft. The impacts on the spacecraft are primarily through charge exchange.

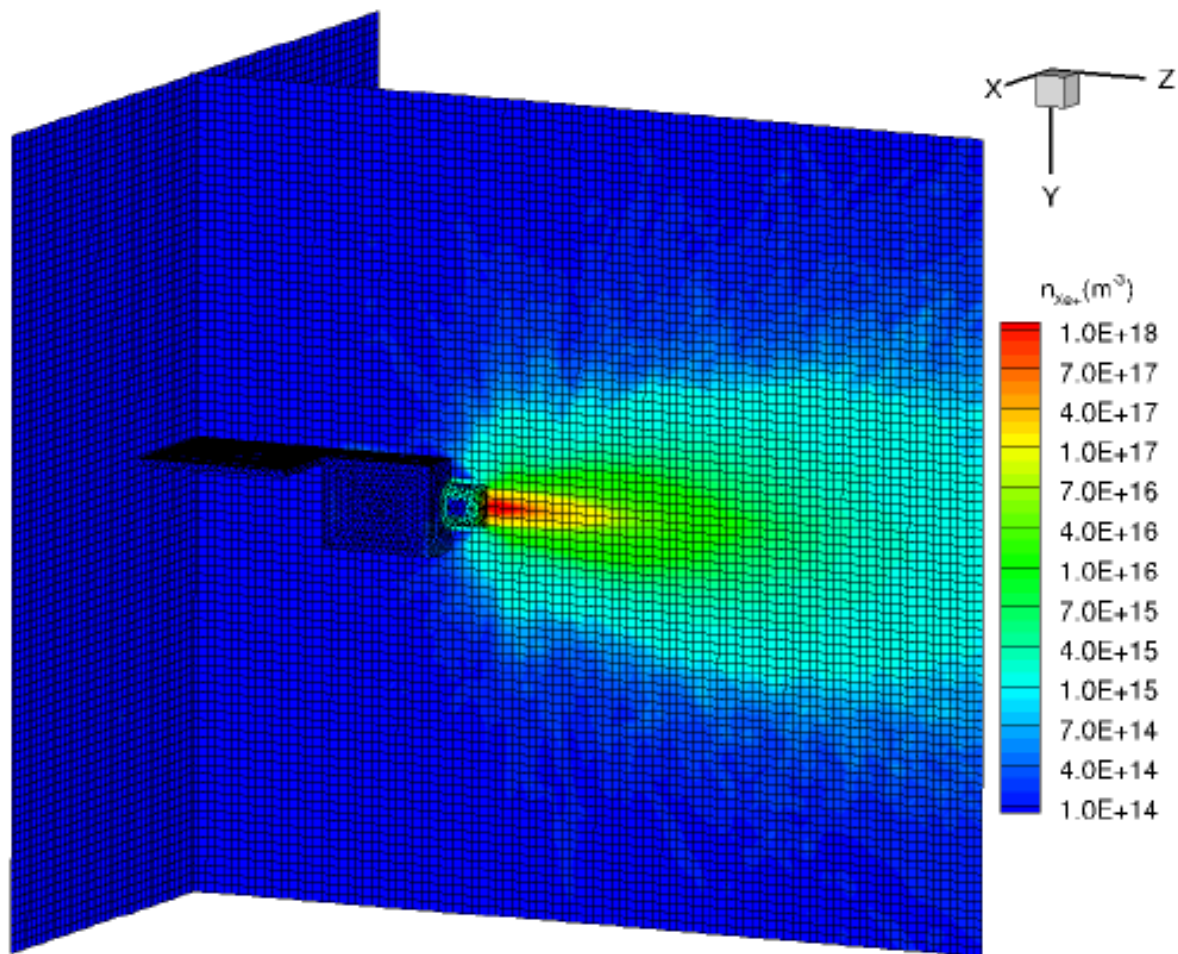


Figure 5: Coliseum Simulation Grid and Thruster Plume Density⁴

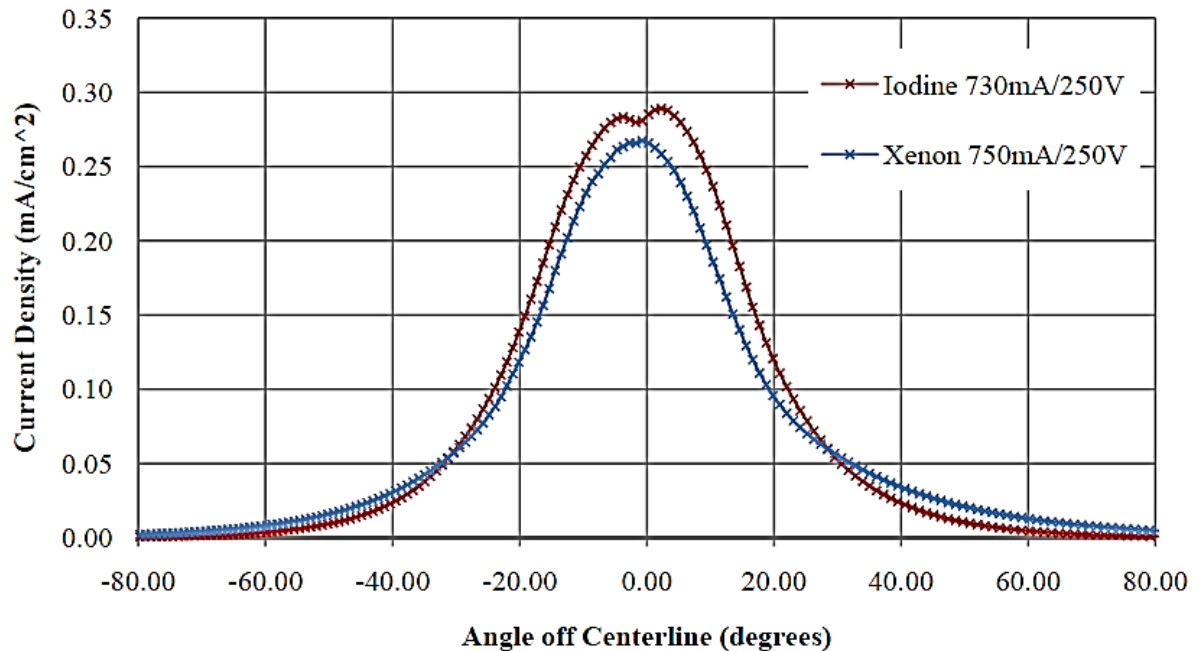


Figure 6: Measured Current Density for Xenon and Iodine, BHT-200, $V_d = 250$ volts²¹

Spacecraft Exposure

The COLISEUM iSAT model (Figure 7) produced flux and density information for the neutrals and ions surrounding the iSAT spacecraft. Figure 7 shows where iodine and iodine plasma interactions will have the greatest impact. The results show we need to be concerned for any materials on the exterior of the satellite, but highest concentrations will be experienced on the thruster side. The thruster face can see iodine and iodine plasma impacts as high as 4.0×10^{19} impacts/m²/s. The thruster mounted surface will be subjected to neutral iodine near 1.0×10^{17} impacts/m²/s and 4.0×10^{18} plasma iodine impacts/m²/s.

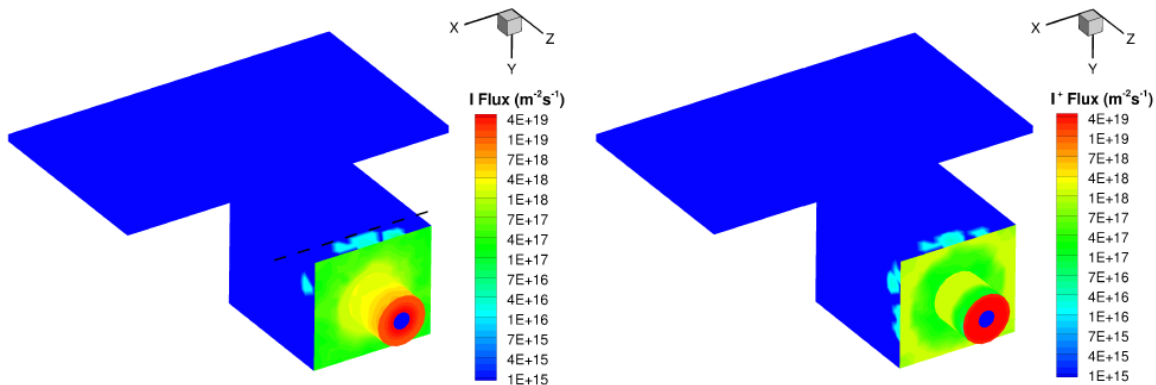


Figure 7: iSAT Plume Interaction⁴

The velocity of both the neutrals and ions impacting the surface will be relatively low. Those ions impacting the spacecraft are produced by high energy impacts of ions in the plume with neutrals. The thermal velocity is 208 m/s for I_2 and 284 m/s for monatomic iodine. The more severe case (higher density) will be for I_2 . For the impact densities seen in the simulation (Figure 7), the following table provides the expected exposure densities.

Table 4: Expected Exposure Densities

	Impacts/m ² /s	Density (#/m ³)
Neutrals	10 ¹⁷	4.8 x 10 ¹⁴
Ions	4.0 x 10 ¹⁸	1.64 x 10 ¹⁶

Deposition is projected to be very low or non-existent for iodine propellant.²² Detailed modeling is required to validate this hypothesis. However, the SERT II mission already demonstrated that condensable propellants are compatible with solar electric propulsion (SEP). Mercury ion engines on SERT II were successfully fired on-orbit for 4000 hours.²³ Most spacecraft surfaces, including solar arrays, were too warm to permit Hg condensation and showed no evidence of condensate.²⁴ Iodine has a much higher vapor pressure than mercury.

The spacecraft exterior will cycle between 73 K (-200°C) (radiator pointing at deep space) to 473 K (200°C) (solar panels in the sun). Operating surface temperatures are nominally 298 K (25°C) to protect the components inside the spacecraft (excluding the solar panels). The iodine will not condense on the surfaces at this temperature and the very low expected pressures of low Earth orbit (Figure 8).

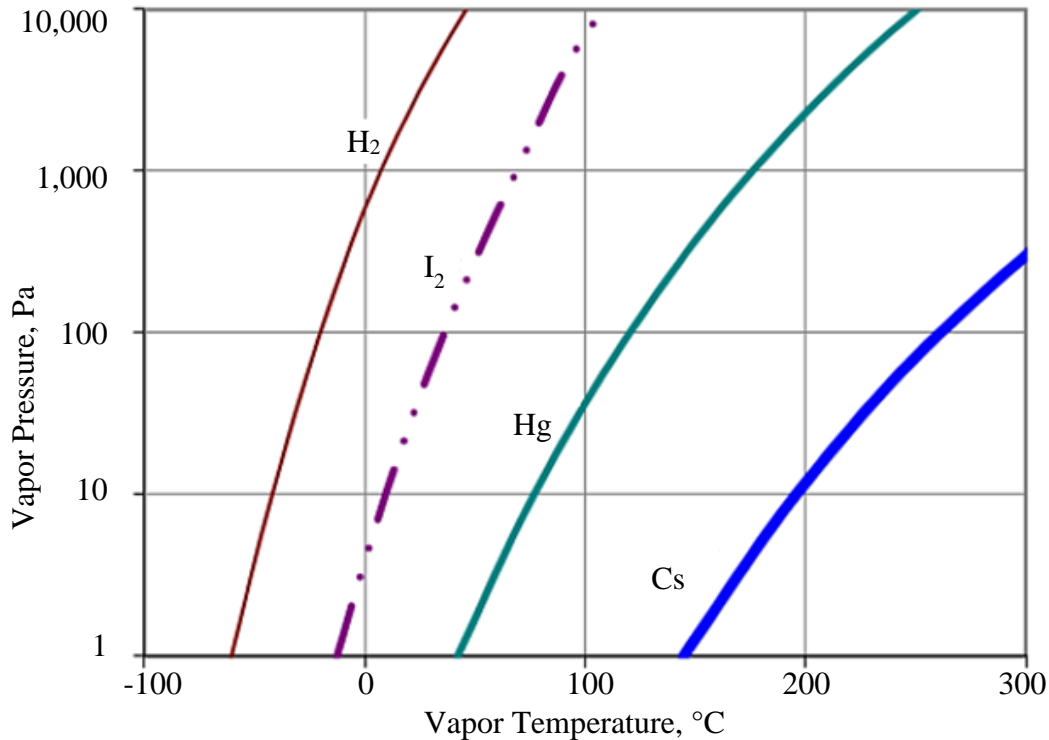


Figure 8: Vapor Pressure of I₂ and Other Electric Propulsion Propellants²⁵

Iodine Feed System

Iodine is a dense solid at low pressures. The current operational design will store propellant below 6,700 Pa.²⁶ Iodine gas can be created thermally and the flow regulated by sublimating the solid at relatively low temperatures (Figure 8 ~100 °C).²⁵ The challenges for the flow system include: producing iodine vapor quickly enough for the thruster, regulating the flow accurately and ensuring the iodine does not condense on the inside of the feed system before reaching the thruster. Polzin and Peeples have demonstrated a feed system capable of producing the iodine flow needed

by the 200 W thruster (Table 3, 0.916 mg/s).²⁶ This feed system identified the need to heat the lines, valves and sensors in direct contact with the iodine. Operating system pressures above 10,000 Pa required the line temperatures set at 473 K (200 °C) to ensure no iodine condensation.

Technical Approach

The technical approach includes three major test campaigns: measure iodine impact on spacecraft materials, measure impact of iodine plasma in space-like conditions, and develop iodine-interaction models for spacecraft materials (chemical reactivity, sputtering, and erosion). Much of the work for the iodine interaction has already been accomplished. The effort to complete this task will be accomplished in conjunction with the second major test campaign, iodine plasma in space-like conditions. To develop the erosion model, the sputtering rates will need to be determined for spacecraft materials exposed to charge-exchange iodine particles.

Iodine Impact and Iodine Plasma in Space-Like Conditions

The iodine exposure analysis will focus on several measurable statistics. These characteristics include: surface roughness/features, adsorption/absorption, and corrosion rate. The samples will be examined using a profilometer and a Scanning Electron Microscope. These instruments will be used to measure the surface features, roughness and overall sample dimensions accurately, before and after exposures. The hope will be to quantify mass loss (surface regression, thickness changes), interstitial diffusion of iodine between grains, iodine deposition, and iodine reactions with surface materials.

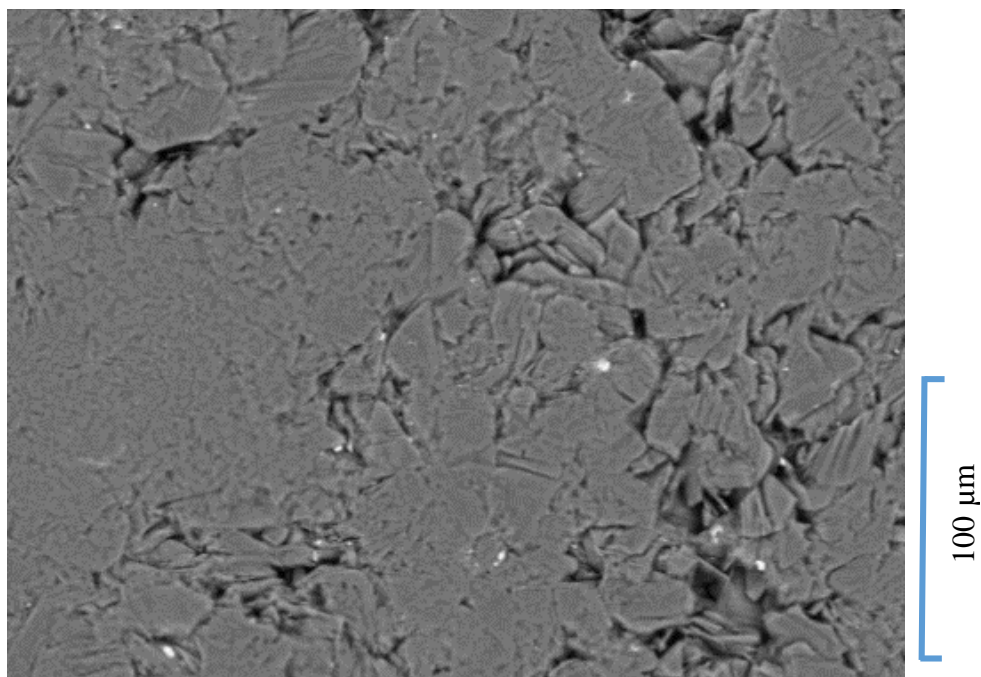


Figure 9: SEM Scan of Boron Nitride Sample

The material samples for this research effort will not be polished. Surface characteristics will be quantified before and after each exposure. The profilometer (capable of sub-micrometer) will be provide any changes in bulk roughness, indicating preferential reactions with the surface. The

changes in surface features will be quantified using the SEM (Figure 9). Specific characteristics determined from SEM will be diffusion of iodine into the grain structure and reactions with the surface. The SEMs at the University of Alabama and NASA/MSFC both have Energy Dispersive X-ray (EDX) capabilities. This capability will provide the emissions spectrum of our samples, indicating if iodine is in the surface. For samples identified as having iodine in the surface, they will be further examined at NASA/MSFC to try and determine whether the iodine is impregnated or reacted with the surface materials.

For the initial exposure tests, square test specimens, approximately 20 mm wide by 0.5 to 1.5 mm thick, were cut from flat sheets of several materials. The thickness of each test specimen was measured before and after iodine exposure with a digital micrometer to an accuracy of ± 0.001 mm.

The material removed from the surface through chemical reactions will be characterized as corrosion rates. The total erosion rates of the material will include both the corrosion rate and the sputtering rate (momentum exchange removal of mass). Corrosion rates of millimeters per year were derived from thickness changes over the tested time. The accuracy of each measurement is determined by the ± 0.001 mm accuracy of the digital micrometer and the test length normalized to one year. For a thirty-day iodine flow exposure, the accuracy of each corrosion rate was 0.012 mm/year. The results of the seven-day iodine bath exposure had an average uncertainty of each corrosion rate of 0.052 mm/year.

The iodine exposure showed iron and copper alloys as having the highest reaction rates. Surprisingly, tantalum and titanium also demonstrated high reaction rates in iodine. The expectation was for these metals to exhibit the same low reaction rates they have with oxygen. Nickel alloys prove to be the most resistant to iodine reactivity.

The complete results of the exposure testing will be published separately.²⁷

Table 5: Corrosion Rates when Exposed to Iodine Gas

Alloy	Flow Exposure, Corrosion Rate	Bath Exposure, Corrosion Rate
	(mm/year)	(mm/year)
6061 Aluminum	0.147	0.209
110 Copper	0.606	
304 Stainless Steel (Iron)	1.055	0.261
Hastelloy C-22 (Nickel)	0.019	0.052
Pure Tantalum		0.834
Commercially Pure Titanium	0.037	0.782

With these environments known, the test plan will include a range of pressures and plasma densities to get an accurate representation of the expected spacecraft exposure. Pressures at 10,000, 300, 0.1 and 0.001 Pa will be considered. Article temperatures for cathode materials will be heated while being exposed to plasma. Current heating capability of the test equipment is 1200 K.

Samples will be identified and indexed to try and make measurements in the same locations before and after the exposure to iodine plasma. Measurable features will be repeated enough times to determine average values with at least a 95% confidence, where appropriate (i.e. surface

roughness). In preparation, all samples will go through the same cleaning process: cleaned with alcohol and sealed. Metal samples will be micro indented to provide an easily identifiable reference when viewed under a Scanning Electron Microscope (SEM).

The anode in Figure 10 (iron) shows the results of the impact on the Busek 200W HET after being operated using iodine. The left image shows a glowing anode just after shutdown. The evidence strongly suggests some negatively ionized plasma (I^- , I_2^-) is being generated and accelerated into the anode surface. The image on the right is the same anode after removal from the thruster. Testing components and hardware exposed to iodine plasma showed no immediate discoloration in the vacuum chamber. However, when the component was exposed to atmosphere for several hours, significant oxidation occurred. Since iron reacts with air after being exposed to iodine plasma, these samples will be handled in an inert environment from the plasma chamber to the SEM chamber. One of the primary goals is to determine the impact iodine is having on the reactivity of iron with air.



Figure 10: Busek 200W HET after Operating on Iodine: Left – Anode Just After Shutdown (Glowing Hot), Right – Anode Extensively Corroded.²¹

The sample materials identified in the following table will be exposed to iodine and to iodine plasma, as indicated. The list of materials is a compilation of expected materials to be used for spacecraft components. This list was created with the collaboration of NASA/MSFC and Busek Co., Inc.

Table 6: Spacecraft Materials to be Tested

Material	Typical Application	Satellite Environment	Plasma
Alumina	Isolator, insulator, low erosion surface	Inside Cathode, Exhaust Plume	Yes
Aluminum, 6061	Structure	Spacecraft Exposure	
Aluminum, 7075	Structure	Spacecraft Exposure	
Aluminum, anodized 7075	Structure	Spacecraft Exposure	
Arathane 5750LV	Urethane composite insulating circuit	Spacecraft Exposure	
AS22759/33 (silver plated copper wire, covered with ETFE)	Lead wire	Spacecraft Exposure	

AS22759/41	Lead wire	Spacecraft Exposure	
BaO-W insert	Cathode emitter	Inside Cathode	Yes
Brass, C260 (Cu-70%:Zn-30%)	Electrical connections	Spacecraft Exposure	
Boron Nitride (AX05, HBC, HP)	Thruster exit rings, anode chamber	Exhaust Plume	Yes
Borosilicate Glass	Solar panel cover	Spacecraft Exposure	
Buna-N (acrylonitrile butadiene rubber)	Seals	Iodine Feed System	
Carbon fiber composite (epoxy resin)	Structure	Spacecraft Exposure	
Cerium Hexaboride, CeB6	Cathode emitter	Inside Cathode	Yes
Copper, 110	Wiring	Spacecraft Exposure	
Cu-Ni 70/30	Propellant isolator	Spacecraft Exposure	
DC 6-1104 (hexamethyl-disilazane reaction with silica)	RTV sealant	Spacecraft Exposure	
EA934NA (Epoxy)	Potting material	Spacecraft Exposure	
Eccobond 104 (epoxy adhesive)	Adhesive	Spacecraft Exposure	
Electride, C12A7 (12CaO*Al2O3(4e ⁻))	Cathode emitter	Inside Cathode	Yes
FeNi42 (NILO alloy 42)	Propellant isolator	Iodine Feed System	
Germanium Coated Black Kapton	Solar Cells	Spacecraft Exposure	
Gold 100 (Braze)	cathode braze	Spacecraft Exposure	
Electroless Nickel over Hipercor 50A	Shunt	Spacecraft Exposure	
Gold over Hipercor 50A	Shunt	Spacecraft Exposure	
Electroless Nickel over CMI Iron	Shunt	Spacecraft Exposure	
Gold over CMI Iron	Shunt	Spacecraft Exposure	
Hasteloy C-22 (Ni-56%:Cr-22%:Mo-13%)	Structure	Spacecraft Exposure	
HPG-83 isomolded graphite	Cathode keeper	Exhaust Plume	Yes
Hipercor 50A (Fe-50%:Co-48%:Va-2.0%)	Electromagnets	Spacecraft Exposure	
Incoloy A286 (Fe-40%:Ni-35%:Cr-20%)	Fasteners	Spacecraft Exposure	
Inconel (Ni-60%:Cr-20%:Fe-10% ...)	BHT200i screens	Spacecraft Exposure	
Indium-Doped Tin Oxide (ITO)	Charge control on solar panels	Spacecraft Exposure	
Kalrez 7075 (perfluoroelastomer, FFKM)	Insulation	Spacecraft Exposure	Yes
Kapton (polyimide)	Free O protection	Spacecraft Exposure	
Kovar (K94610), 0.02 max. C, 0.30 Mn, 0.20 Si, 29.00 Ni, 17.00 Co, Bal. Fe	Propellant isolator	Spacecraft Exposure	
Lanthanum Hexaboride, LaB6	Cathode emitter	Inside Cathode	Yes
MACOR (46% SiO2, 17% MgO, 16% Al2O3, 10% K2O, 7% B2O3, 4% F)	Cathode components	Inside Cathode	Yes
Magnesium Fluoride (MgF2)	Solar panels	Spacecraft Exposure	
MLI (exposed layer is beta cloth, finely woven silica fibers OR ITO)	Spacecraft insulation	Spacecraft Exposure	
Mo/Re 48	Cathode	Inside Cathode	Yes
Molybdenum	Cathode	Inside Cathode	Yes
Molybdenum TZM (0.50% Ti, 0.08% Zr, 0.02% C, balance Mo)	Propellant supply junction	Spacecraft Exposure	

Moly-Manganese Metallized Surface	Metalized alumina ceramic prior to braze	Spacecraft Exposure	
Nickel	Structure	Spacecraft Exposure	
Nichrome 80/20 Alloy	Structure	Spacecraft Exposure	
Palniro4 (AMS-4785), Au-50%:Ni-25%:Pd-25%	Cathode braze	Spacecraft Exposure	
Polyether ether ketone (PEEK, thermoplastic)	Seals	Iodine Feed System	
Platinum	Cathode heat shield	Inside Cathode	Yes
PPO (p-phenylene oxide, thermoplastic)	Seals	Iodine Feed System	
PPS (Polyphenylene Sulfide, organic polymer)	Seals	Iodine Feed System	
PTFE (Teflon)	Supply tubing, valves	Iodine Feed System	
Reltek B-4811 (epoxy resin)	Potting electronics	Spacecraft Exposure	
Rhenium	Alt. cathode heater	Inside Cathode	Yes
Rulon XL (Poly Tetra Fluoro-Ethylene)	Seals	Iodine Feed System	
Scotchweld 2216 B/A (epoxy resin)	Potting electronics	Spacecraft Exposure	
Silver Coated Teflon (AGT5, Ag-FEP)	Thermal control surface (radiator)	Spacecraft Exposure	
Soda-lime glass (74% SiO ₂ , 13% Na ₂ O, 8% CaO, 4% MgO, 1% other oxide)	Solar panels, instruments	Spacecraft exposure	
Stainless Steel 304 (Fe-74%:Cr-18%:Ni-8%)	Thruster structure	Spacecraft Exposure	
Stainless Steel 316 (Fe-68%:Cr-18%:Ni-12%:Mo-2%)	Structure	Spacecraft Exposure	
Steel, 4130 (low-C Mo-Cr steel), mostly Fe	Structure	Spacecraft Exposure	
Stycast thermally conductive epoxy	Remove heat from electronics	Spacecraft Exposure	
Tantalum	Cathode heat shield	Inside Cathode	Yes
Teflon PFA 950HP Plus (fluoroplastic)	Propellant lines	Iodine Feed System	
Tefzel ETFE (ethylene-tetrafluoroethylene)	Wire coatings	Spacecraft Exposure	
Titanium Grade 1, 2 (pure Ti)	Structure	Spacecraft Exposure	
Titanium grade 5, Ti 6Al-4V	Structure	Spacecraft Exposure	
Tungsten - 2% Thoriated or Lanthanated	High temp plasma	Inside Cathode	Yes
Tungsten	Cathode internal	Inside Cathode	Yes
Ultem 2300, 3000 (Polyetherimide resin)	Potting electronics	Spacecraft Exposure	
Vacuum grade braze BVAg-8 (Cusil), Ag-72%:Cu-28%	Propellant isolator braze	Spacecraft Exposure	
Vacuum grade braze BVAu-4 (Nicro), Au-82%:Ni-18%	Propellant isolator braze	Spacecraft Exposure	
Vespel (polyimide, thermoplastic)	Seals	Iodine Feed System	
Viton (fluoropolymer elastomer)	Seals	Iodine Feed System	

Sputtering Impacts of Iodine

Most of the momentum exchange damage to spacecraft surfaces is caused by low-energy, charge-exchange plasma. Therefore, sputter rate values are primarily needed in the energy range between 50 and 300 eV.²⁸

The test program needs to determine dependencies on both angle and dependencies. Using the Kannenberg approach, the sputter models will capture sputter rates at incidence angles 0°, 20°, 40°, 60°, and 80° and ion energies 50, 100, 300, 500, and 2,000 eV for each of the materials shown in the table.

Experimental Setup

Iodine and Iodine Plasma

The following description focuses on the specific experimental setup at NASA/MSFC facility. Similar components are being utilized at the University of Alabama. The experiment is constructed beneath a fume hood. A water cooled cylindrical quartz tube serves as the plasma confinement tube and is inserted into a Mellen NACCI tube furnace. A coil (RF antenna) is placed around the quartz tube on one end. The tube is sealed by a vacuum flange assembly. In order to provide RF shielding, the frame of a metal box was constructed and placed over the antenna end of the tube. The inside and outside of the box was wrapped in silver coated FEP Teflon®. The other end of the quartz tube was connected via a vacuum sealing flange assembly to flexible wire reinforced PVC vacuum line. This line was connected to a water-cooled cold trap to prevent iodine vapor from escaping and damaging the vacuum pump. The vacuum line is connected to the vacuum pump via an oil trap placed on the vacuum pump intake port. In addition to the oil mist filter, a charcoal exhaust filter is installed on the vacuum pump exhaust port to further reduce the potential of iodine exhaust contamination. This exhaust is pumped into the fume hood.

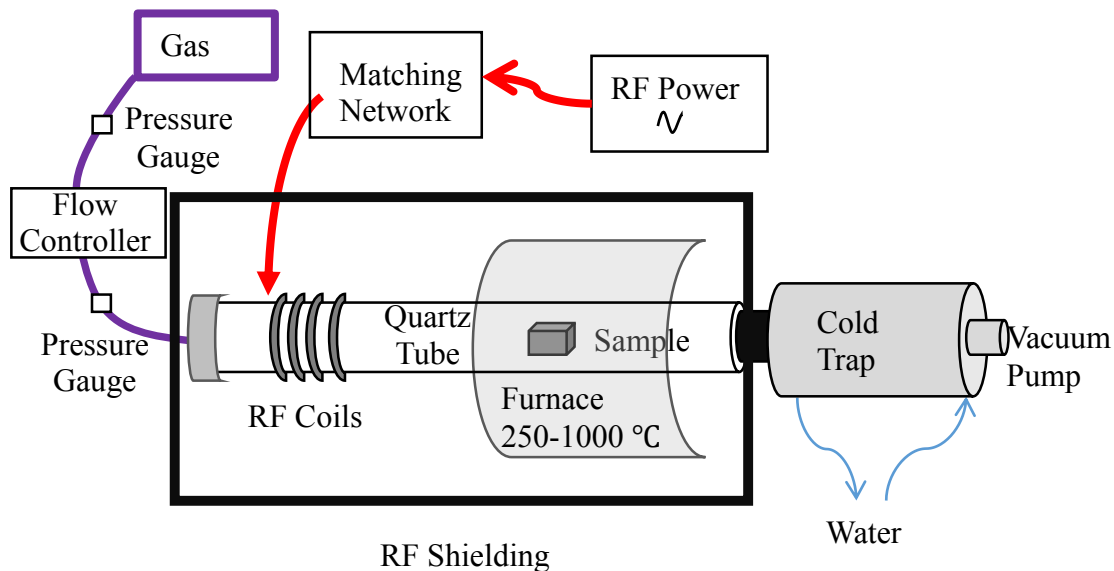


Figure 11: Test Setup, Plasma Source

Total pressure is measured accurately of 0.1 Pa at NASA/MSFC (Inficon PCG554, Pirani and capacitance diaphragm gauge) and with an accuracy of 1.0×10^{-4} Pa at the University of Alabama (Oerlikon Leybold PTR 90N, cold cathode ion gauge). Temperatures are monitored at several

locations in the test setup using thermocouples and IR sensors: iodine entering the chamber, the test article, quartz tube, exhaust, RF antenna.

Experimental Iodine Feed System

The iodine feed system has already demonstrated operation at NASA/MSFC. Components are on hand and ready to integrate at the University of Alabama.

Iodine flow testing conducted at NASA/MSFC (Dr. Gregory Jerman) used a standard quartz vacuum tube furnace at a pressure of 10,000 Pa to simulate low pressure iodine vapor exposure in a vacuum. The furnace hot zone temperature set point was 473 K (200 °C), the maximum temperature expected for the iodine feed system. Iodine vapor was generated by heating solid iodine to 348 K (75°C) in an argon atmosphere. The iodine vapor pressure is approximately 2,000 Pa when mixed with argon at 200,000 Pa.²⁹ The combined iodine vapor and argon gas then flowed through a flow control valve that regulated the pressure in the vacuum tube furnace to 10,000 Pa. The flow control valve and connected tubing were heated to 373 K (100°C) to minimize condensation of iodine during test operations.

The experimental feed system can accurately control the iodine density and pressure expected by the spacecraft propellant feed system. Argon will not be available on the spacecraft. Further exposure tests will be performed without using an argon carrying gas.

Parameters of interest with respect to the feed system include iodine flow rate, exposure time, and sample temperature. Two test conditions have been demonstrated for the current results: flow exposure → 10,000 Pa at 373 K for extended exposure times (30 days) and bath exposure → 100,000 Pa at 373 K for seven days.

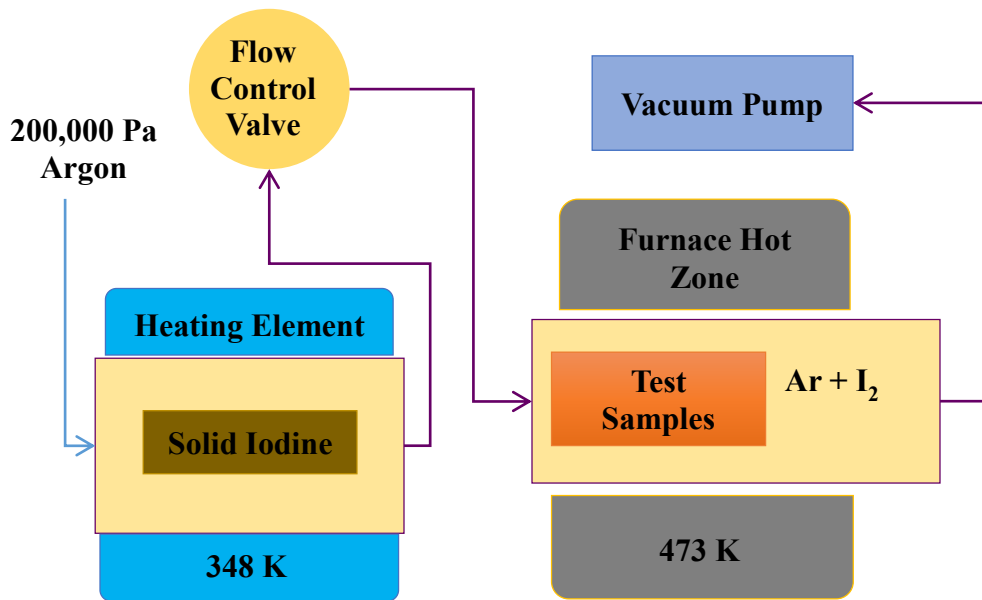


Figure 12: Iodine Flow Exposure Test Setup

Plasma Generation

The RF coils in Figure 11 deliver the radio frequency energy to the mass inside the quartz tube. In order to efficiently deliver the RF energy from the RF power supply, an adjustable matching network was constructed. The available RF power supplies currently provide 13.56 MHz, 600 W (NASA/MSFC) and 2.0 MHz, 1000 W (University of Alabama). In order to deliver maximum

power, the power source and RF coil impedance must match. The differing RF frequencies required the matching network to have a wide range of operability.

Matching networks are used extensively to match power source impedance with the load (antenna for this research). The impedance is the effective resistance (composed of both Ohmic resistance and reactance) of an electric circuit or component to alternating current. Inductors and capacitors are reactive components and are often employed for matching. Two basic configurations are the Pi and T matching network. The T matching network has only one capacitor leg to ground and acts like a low-pass or high-pass filter, depending on the location of the inductor. The circuit flows through both a capacitor and inductor. The inductor is placed facing (closest) the lower impedance in order to match the circuit. For our research, the antenna proved to be at a lower impedance than the power supply (Figure 13)

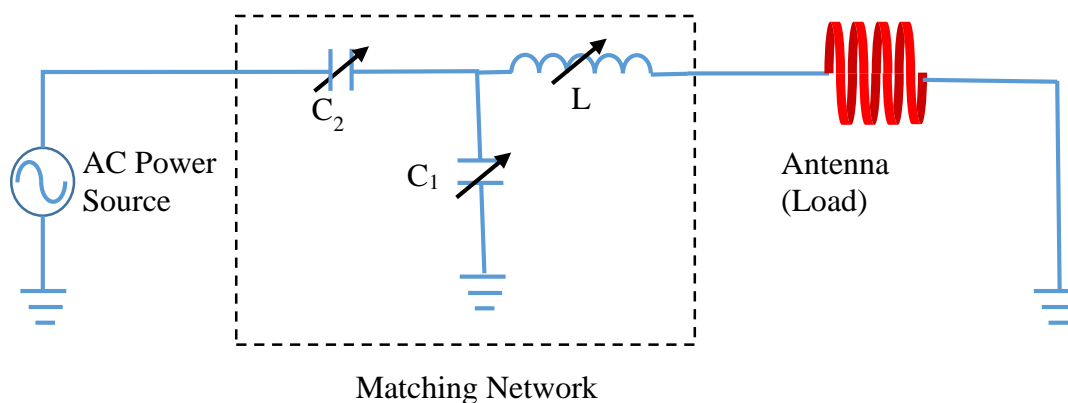


Figure 13: T Matching Network, Inductor Facing Load

The circuits used in this research employs variable capacitors for each leg and a fixed inductor. Several inductors were constructed of various inductance in order to better match the frequency of the AC power source. For 13.56 GHz, lower impedance and capacitance values were required.

Verifiably Measuring Plasma Properties

In order to characterize the performance of our ion source, we will need to measure several characteristics of plasma reliably and accurately. The available plasma probes are capable of measuring the plasma properties and particle fluxes in an ion satellite thruster fairly accurately, but need to be placed into the plasma. The specific diagnostic tools available for this research are the Langmuir probe, Faraday Cup, Retarding Potential Analyzer, and Wein Filter (ExB) probe. The Langmuir probe can determine electron temperature, plasma potential, floating potential, and number densities. The Faraday cup measures ion current densities from ion and plasma sources. Ion current density measurements can be used to calculate ion and plasma source parameters such as beam uniformity, beam symmetry, total energetic particle flux through a given plane, beam divergence, beam centroid, and thrust vector direction. The ExB probe (or Wein filter) has the ability to separate ions according to their energy (E), mass (m), and charge state (z). The electrostatic analyzer (ESA) is designed to separate ions according to their energy to charge ratio (E/z).

The most accurate approach to provide data for the satellite designer is to produce the same iodine plasma environment expected to be experienced by the spacecraft. Szabo and Hillier have

measured exhaust plume characteristics of the BHT-200 using the instruments mentioned in the previous paragraph.^{21,22} For this research effort, the plasma source will have to first be characterized in order to produce the expected plume plasma (Figure 14, Table 7).

Table 7: Species Concentrations for Iodine and Xenon from a BHT-200 HET³⁰

Species	Mol Fraction	Species	Mol Fraction
I_2^+	0.029	Xe^+	0.975
I^+	0.953	Xe^{2+}	0.021
I^{2+}	0.015	Xe^{3+}	0.004

Iodine has overlapping energy states. I^+ , theoretically, has the same energy level (charge per unit mass) as I_2^{2+} . I_2^{2+} is not a stable species, though. The previous research was not able to distinguish if the plasma plume included appreciable amounts of I_2^{2+} . The ESA will be able to better resolve the differences.³¹

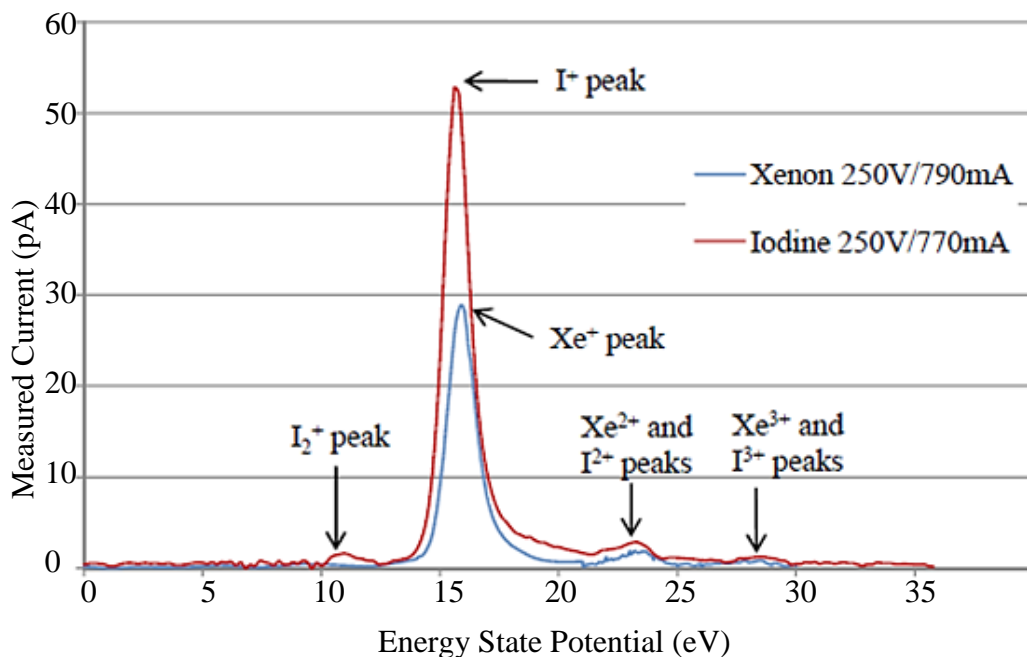


Figure 14: Energy States, ExB Probe, Xenon and Iodine, Plume Centerline²¹

Momentum Exchange (Sputtering)

The Kannenburg model requires data for sputter rates at incidence angles 0°, 20°, 40°, 60°, and 80° and ion energies 50, 100, 300, 500, and 2,000 eV to produce the needed coefficients. In order to generate these energy levels, an additional power supply will be added to the test setup in Figure 11. This power supply will be used to apply a potential difference between the plasma and the sample. The potential difference will be able to accelerate the ions to each of the ion energy levels accurately. Several samples will be used for this phase of the testing in order to provide repeatable results as well as to capture the incident angle influence.

Both xenon and iodine will be used to perform this phase of determining the overall erosion model. The iodine result will be affecting the samples both chemically as well as mechanically (sputtering). The xenon will only be mechanically removing material from the surface. The results

of this testing campaign will determine if the chemical removal of surface material affects the momentum exchange removal of mass.

Collaboration

Air Force Research Lab, Propulsion Directorate (Dr. William Hargus) has extensive experience with plasma diagnostics and space plasma thrusters. Dr. Hargus has agreed to advise and participate in this research effort. AFRL and the University of Alabama now have an Educational Partnership Agreement in place.

Air Force Institute of Technology (Dr. Carl Hartsfield) is loaning the University of Alabama equipment to be used with the ion source. Dr. Hartsfield will be collaborating on this research effort. AFIT and the University of Alabama now have an Educational Partnership Agreement in place.

NASA/MSFC (Kurt Polzin, John Dankanich, and Dr. Gregory Jerman) has installed and is characterizing a propulsion vacuum facility at MSFC specifically to quantify iodine Hall Effect Thruster interactions on spacecraft. They have agreed to advise on this research project and will ensure our testing facilities are properly configured for testing iodine and capturing high quality data.

Busek Co., Inc. (James Szabo and Bruce Pote) has been working with iodine since our first experiments together in 2010. Their continued effort has proved fruitful and will prove to be a valuable resource. They have agreed to advise on this research effort as well.

The project also requires a significant amount of internal collaboration within the University of Alabama. Currently, the UA Micro-Fabrication Facility (MFF) has a micro profiler. The researchers on this proposal will first be making measurements using this profiler. Additionally, surface mapping with the Scanning Electron Microscope will be accomplished in the Central Analytical Facility. The Department of Metallurgy and Materials acquired these instruments.

References and Citations

- ¹ Kieckhafer, A., and King, L. B., "Energetics of Propellant Options for High-Power Hall Thrusters," *Proceedings of the Space Nuclear Conference*, San Diego, CA, 2005.
- ² Hillier, A., Branam, R., Huffman, R., Szabo, J. and Paintal, S., "High Thrust Density Propellants in Hall Thrusters," *49th AIAA Aerospace Sciences Meeting including the New Horizons Forum and Aerospace Exposition*, Orlando, Florida, Jan. 4-7, 2011.
- ³ Dankanich, J., Polzin, K., Calvert, D., Kamhawi, H., "The Iodine Satellite (iSAT) Hall Thruster Demonstration Mission Concept and Development," *50th AIAA/ASME/SAE/ASEE Joint Propulsion Conference*, July 28-31, 2014.
- ⁴ Choi, M., "Modeling iSAT Surface-Plume Interactions," Ph.D. Dissertation, University of Michigan, Ann Arbor, MI, 2016.
- ⁵ Dressler, R., Chiu, Y., and Levandier, D., "Propellant Alternatives for Ion and Hall Effect Thrusters," *38th Aerospace Sciences Meeting and Exhibit*, 2000.
- ⁶ Kannenberg, K., Khayms, V., Hu, S.H., Emgushov, B., Werthman, L., and Pollard, J., "Validation of a Hall thruster plume sputter model," *37th Joint Propulsion Conference*, Salt Lake City, UT, 8-11 July 2001.
- ⁷ Spicer, R. L. "Validation of the Draco Particle-In-Cell Code Using Busek 200W Hall Thruster Experimental Data," M.S. Thesis, Department of Aerospace and Ocean Engineering, Virginia Polytechnic Institute and State University Blacksburg, 2007.
- ⁸ Goebel, D., Watkins, R. and Jameson, K., "LaB6 Hollow Cathodes for Ion and Hall Thrusters," *Journal of Propulsion and Power*, Vol 23, Issue 3, 2007, pp. 552-558.
- ⁹ Warner, D. J., Branam, R.D. and Hargus, W.A., "Ignition and Plume Characteristics of Low-Current Cerium and Lanthanum Hexaboride Hollow Cathodes," *Journal of Propulsion and Power*, Vol. 26, Issue 1, 2010, pp. 130-134.
- ¹⁰ Rand, L.P., "A Calcium Aluminate Electride Hollow Cathode," Ph.D. dissertation, Colorado State University, Fort Collins, CO, 2014.
- ¹¹ Katz, I., Anderson, J. Polk, J., and Brophy, J., "One-Dimensional Hollow Cathode Model," *Journal of Propulsion and Power*, Vol. 19, No. 4, 2003, pp. 595-600.
- ¹² Goebel, D. and Katz, I., *Fundamentals of Electric Propulsion: Ion and Hall Thrusters*, John Wiley & Sons Inc., Hoboken, NJ, 2008, Ch. 5.
- ¹³ Reid, R. C., Prausnitz, J. M., and Sherwood, T. K., *The Properties of Gases and Liquids*, 3rd ed., McGraw-Hill, New York, 1977, pp. 402, 403.
- ¹⁴ Jantz, B., "Contamination and Erosion of the Tacsat-2 Satellite Structure from a 200-Watt Hall Thruster," M.S. Thesis, Department of Aeronautics and Astronautics, Air Force Institute of Technology, Dayton, OH, March 2007.
- ¹⁵ VanGilder, D.B., Fife, J.M., and Gibbons, M.R., "COLISEUM: An Application Programming Interface for Three-Dimensional Plasma Simulations," *JANNAF*, 2003.
- ¹⁶ Fife, J.M., Gibbons, M.R., Hargus, W.A., VanGilder, D.B., Kirtley, D.E., and Johnson, L.K., "The Development of a Flexible, Usable Plasma Interaction Modeling System," *38th AIAA/ASME/SAE/ASEE Joint Propulsion Conference*, Indianapolis, IN, 7-10 July, 2002.
- ¹⁷ Dietrich, S. and Boyd, I.D., "Scalar and Parallel Optimizes Implementation of the Direct Simulation Monte Carlo Method," *Journal of Computational Physics*, Vol. 126, 1996, pp. 228-243.
- ¹⁸ VanGilder, D.B., Boyd, I.D., and Keidar, M., "Particle Simulations of a Hall Thruster Plume," *Journal of Spacecraft and Rockets*, Vol. 37, No. 1, 2000.
- ¹⁹ Hargus, W. A., and Charles, C. S., "Near Exit Plane Velocity Field of a 200-Watt Hall Thruster." *Journal of Propulsion and Power*, Vol. 24, No. 1, 2008, pp. 127-133.

-
- ²⁰ Ali, A and Kim, Y., "Ionization Cross Sections by Electron Impact on Halogen Atoms, Diatomic Halogen and Hydrogen Halide Molecules," *Journal of Physics B: Atomic, Molecular, and Optical Physics*, Vol. 41, 2008 pp. 145202 -145214.
- ²¹ Hillier, A.C., "Revolutionizing Space Propulsion Through the Characterization of Iodine as Fuel for Hall-Effect Thrusters," M.S. Thesis, Department of Aeronautics and Astronautics, Air Force Institute of Technology, Dayton, OH, March 2011.
- ²² Szabo, J., Robin, M., Paintal, S., Pote, B., Hruby, V., Freeman, C., "Iodine Plasma Propulsion Test Results at 1-10 kW," *IEEE Transactions on Plasma Science, Special Issue – Plasma Propulsion*, Vol. 43, No. 1, 2015, pp. 141-148.
- ²³ Kerslake, W., and Ignaczak, L. "Development and Flight History of SERT II spacecraft," *28th AIAA/SAE/ASME/ASEE Joint Propulsion Conference and Exhibit*, AIAA-92-3516, July 1992.
- ²⁴ Hall, D., Newnam, B, Womack, J., "Electrostatic Rocket Exhaust Effects on Solar-Electric Spacecrafts," *Journal of Spacecraft*, Vol. 7, No. 3, March 1970, pp. 305-312.
- ²⁵ *CRC Handbook of Chemistry and Physics*, 83rd Edition, CRC Press LLC, Boca Raton, FL, 2002.
- ²⁶ Polzin, K. and Peeples, S., "Hall Thruster Propellant Feed Ssystem for a CubeSat," *50th AIAA/ASME/SAE/ASEE Joint Propulsion Conference*, Cleveland, OH, July 28-30, 2014.
- ²⁷ Jerman, G., "iSAT Material Test Results," NASA Marshall Space Flight Center, August 2016.
- ²⁸ Khayms, V., Kannenberg, K., Meyer, J. W., & Werthman, L., "Overview of Hall current thruster integration activities at Lockheed Martin Space Systems company," *27th International Electric Propulsion Conference*, Pasadena, CA, 2002.
- ²⁹ Lync, C. T., *CRC Handbook of Materials Science*, Vol. 1, p. 79, CRC Press Inc., Boca Raton, FL, 1974.
- ³⁰ Szabo, J., Pote, B., Paintal, S., Robin, M., Hillier, A., Branam, R. D., and Huffmann, R. E., "Performance Evaluation of an Iodine-Vapor Hall Thruster." *Journal of Propulsion and Power*, Vol. 28, No. 4, 2012, pp. 848-857.
- ³¹ Szabo, J. and Robin, M., "Plasma Species Measurements in the Plume of an Iodine Fueled Hall Thruster," *Journal of Propulsion and Power*, Vol. 30, No. 5, September–October 2014, pp.1357-1367.

AFOSR Deliverables Submission Survey

Response ID:7317 Data

1.

Report Type

Final Report

Primary Contact Email

Contact email if there is a problem with the report.

rdbranam@eng.ua.edu

Primary Contact Phone Number

Contact phone number if there is a problem with the report

9376812943

Organization / Institution name

The University of Alabama

Grant/Contract Title

The full title of the funded effort.

Iodine as an Alternative Fuel for Electric Propulsion

Grant/Contract Number

AFOSR assigned control number. It must begin with "FA9550" or "F49620" or "FA2386".

FA9550-15-1-0371

Principal Investigator Name

The full name of the principal investigator on the grant or contract.

Richard D. Brnaam

Program Officer

The AFOSR Program Officer currently assigned to the award

Mitat Birkan

Reporting Period Start Date

09/15/2015

Reporting Period End Date

09/14/2016

Abstract

Initial mission profile studies have shown iodine will enable micro-satellites to accomplish several Air Force missions using much smaller, cheaper satellites; orbit raising, deorbiting, rendezvous, maintenance mission, orbital debris removal, retrieval of errant spacecraft. Iodine imparts volume-constrained spacecraft with up to three times the impulse compared to existing space propulsion systems (i.e. Hall Effect Thruster with xenon). Iodine is stored as a solid (no high pressure vessels), at density three times those of xenon (impulse density two to three times). Iodine presents unique challenges, though. This research addressed the impact of iodine on solar panel surfaces, spacecraft structures and sensitive instruments on board satellites by providing predictive computational tools to satellite designers. Accumulation of iodine film on spacecraft surfaces will present several unique issues: chemical erosion and iodine adsorption/absorption. Of particular concern would be shorting dielectric surfaces, changing radiator emissivities, and damaging optical coatings. To date, chemical reactivity and chemical erosion of iodine with several satellite materials (steel, aluminum, tantalum, etc.) have been determined and tested.

Distribution Statement

This is block 12 on the SF298 form.

DISTRIBUTION A: Distribution approved for public release.

Explanation for Distribution Statement

If this is not approved for public release, please provide a short explanation. E.g., contains proprietary information.

SF298 Form

Please attach your [SF298](#) form. A blank SF298 can be found [here](#). Please do not password protect or secure the PDF. The maximum file size for an SF298 is 50MB.

[sf0298_Branam.pdf](#)

Upload the Report Document. File must be a PDF. Please do not password protect or secure the PDF. The maximum file size for the Report Document is 50MB.

[Iodine+as+an+Alternative+Fuel+for+Electric+Propulsion+FINAL.pdf](#)

Upload a Report Document, if any. The maximum file size for the Report Document is 50MB.

Archival Publications (published) during reporting period:

New discoveries, inventions, or patent disclosures:

Do you have any discoveries, inventions, or patent disclosures to report for this period?

No

Please describe and include any notable dates

Do you plan to pursue a claim for personal or organizational intellectual property?

Changes in research objectives (if any):

Change in AFOSR Program Officer, if any:

Extensions granted or milestones slipped, if any:

AFOSR LRIR Number

LRIR Title

Reporting Period

Laboratory Task Manager

Program Officer

Research Objectives

Technical Summary

Funding Summary by Cost Category (by FY, \$K)

	Starting FY	FY+1	FY+2
Salary			
Equipment/Facilities			
Supplies			
Total			

Report Document

Report Document - Text Analysis

Report Document - Text Analysis

Appendix Documents

2. Thank You

E-mail user

Dec 05, 2016 14:20:06 Success: Email Sent to: rdbranam@eng.ua.edu